Central European Science Journals
w w w . c e s j . c o m

Central European Journal of Physics
Central European Science Journals
CEJP 2(1) 2004 220–240

Critical fields of a superconducting cylinder

G. F. Zharkov

P.N. Lebedev Physical Institute,
Russian Academy of Sciences,
Leninsky pr., 53, 119991 Moscow, Russia

Received 7 July 2003; accepted 4 November 2003

Abstract: The self-consistent solutions of the nonlinear Ginzburg–Landau equations, which describe the behavior of a superconducting mesoscopic cylinder in an axial magnetic field H (provided there are no vortices inside the cylinder), are studied. Different vortex-free states (M-, e-, d-, p-), which exist in a superconducting cylinder, are described. The critical fields (H_1, H_2, H_p, H_i, H_r), at which the first or second order phase transitions between different states of the cylinder occur, are found as functions of the cylinder radius R and the GL-parameter $\varkappa$. The boundary $\varkappa_c(R)$, which divides the regions of the first and second order (s,n)-transitions in the icreasing field, is found. It is found that at $R \to \infty$ the critical value is $\varkappa_c = 0.93$. The hysteresis phenomena, which appear when the cylinder passes from the normal to superconducting state in the decreasing field, are described. The connection between the self-consistent results and the linearized theory is discussed. It is shown that in the limiting case $\varkappa \to 1/\sqrt{2}$ and $R \gg \lambda$ (λ is the London penetration length) the self-consistent solution (which correponds to the so-called metastable p-state) coincides with the analitic solution found from the degenerate Bogomolnyi equations. The reason for the existence of two critical GL-parameters $\varkappa_0 = 0.707$ and $\varkappa_c = 0.93$ in bulk superconductors is discussed.

Keywords: GL-equations, critical fields, hysteresis
PACS (2000): 74.25.-q, 74.25.Dw

1 Introduction

According to the macroscopic Ginzburg–Landau theory [1] all superconductors can be divided in two groups (or types) corresponding to the magnitude of their material parameter $\varkappa$ [$\varkappa < \varkappa_0$ (type-I), or $\varkappa > \varkappa_0$ (type-II), where $\varkappa_0 = 1/\sqrt{2} = 0.707$]. Such division reflects the fact that the surface free energy σ_{ns} vanishes (if $\varkappa = \varkappa_0$ [1]) at the interface between two semi-infinite metallic phases (normal, n-, and superconducting, s-), which

are in equilibrium in a magnetic field. For $\varkappa > \varkappa_0$ the value $\sigma_{ns} > 0$, which points to the instability of the n-phase relative to the formation of the s-phase inside the bulk type-I superconductor. The existence of the critical parameter $\varkappa_0$ is mentiond in all text books [2–5] as the important result of the GL-theory.

We recall, however, that the value $\varkappa_0 = 1/\sqrt{2}$ was found in [1] for the infinite system (assuming no vortices inside the superconductor). In the case of a finite dimension superconductor the situation turns out to be much more complicated. For instance, the behavior of a plate [6] of sufficiently small thickness D in a magnetic field H (even in the simplest vortex-free state) is far from trivial. Basing on the self-consistent solutions of the GL-equations [6], the thickness-dependent critical parameter $\varkappa_c(D)$ was found (with $\varkappa_c(D) \to 0.93$ when $D \to \infty$), which separates two groups (or classes) of the behavior of the plate magnetization $M(H)$ (we use the notation $\overline{B} = H + 4\pi M$, where $\overline{B}$ is the mean field value in the specimen, H is the external field). For $\varkappa < \varkappa_c(D)$ (i.e., in class-I superconductors) the plate magnetization vanishes abruptly at some field H_1 (by a first order transition from s- to n-state, if the field H increases). For $\varkappa > \varkappa_c(D)$ (i.e., in class-II superconductors) a second order phase transition takes place. The hysteresis phenomena, which accompany the plate transitions from n- to s-states in a decreasing field H, were also studied. It was shown, that in a field decreasing regime there exists another D-dependent GL-parameter, which for large D coincides with $\varkappa = 1/\sqrt{2}$. In addition, the critical fields H_1, H_2, H_p and H_r were also found, which correspond to the transitions between different possible states of the plate (such as e-, d-, p-, M-, n-states [6, 7]).

In the present paper the corresponding study is made for a long superconducting cylynder of radius R, placed in an axial magnetic field H. The behavior of the cylinder and the plate in the vortex-free state are qualitatively analogous. Moreover, the cylinder's geometry was already considered in [8–11]; however, some essential details of the general picture in [8–11] are missing. The main attention is devoted below to the questions not discussed earlier; to facilitate the reading of the paper and set the problem in context some important concepts for the understanding will be briefly recalled.

2 Equations

The GL-equations for the order parameter ψ and φ-component of the potential vector A can be written in the cylidrical co-ordinate system (r, φ, z) in a form

$$\frac{d^2a}{d\rho^2} - \frac{1}{\rho}\frac{da}{d\rho} - \frac{\psi^2}{\varkappa^2}a = 0, \tag{1}$$

$$\frac{d^2\psi}{d\rho^2} + \frac{1}{\rho}\frac{d\psi}{d\rho} + (\psi - \psi^3) - \frac{a^2}{\rho^2}\psi = 0. \tag{2}$$

Here $\psi(\rho)$ is a real function $(0 \le \psi \le 1)$, $\rho = r/\xi$ is a dimensionless co-ordinate, $a(\rho)$ is

the dimensionless magnetic field potential, while

$$A = \xi H_\xi \frac{a}{\rho}, \quad b = \frac{B}{H_\xi} = \frac{1}{\rho}\frac{da}{d\rho}, \quad H_\xi = \frac{\phi_0}{2\pi\xi^2},$$

ξ is the coherence length, $\lambda = \varkappa\xi$ is the London penetration depth, $\varkappa$ is the GL-parameter, H_ξ is the unity for measuring the field, $\phi_0 = hc/2e$ is the flux quantum. The boundary conditions to Eqs. (1), (2) are

$$a|_{\rho=0} = 0, \quad \left.\frac{1}{\rho}\frac{da}{d\rho}\right|_{\rho=R_\xi} = h_\xi, \tag{3}$$

$$\left.\frac{d\psi}{d\rho}\right|_{\rho=0} = 0, \quad \left.\frac{d\psi}{d\rho}\right|_{\rho=R_\xi} = 0, \tag{4}$$

where $R_\xi = R/\xi$ and $h_\xi = H/H_\xi$. The magnetic moment (or the cylinder magnetization) $M_\xi = M/H_\xi$ is found from the formula $\overline{b} = h_\xi + 4\pi M_\xi$, where $\overline{b} = \overline{B}/H_\xi = 2a(R_\xi)/R_\xi^2$, the overline means the averaging over the specimen volume.

The difference of the Gibbs free energies in superconducting and normal states, Δg [related to the unity volume and normalized by $H_{cb}^2/8\pi$, where $H_{cb} = \phi_0/(2\pi\sqrt{2}\lambda\xi)$], is expressed through the system magnetic moment [12]:

$$\Delta g = g_0 - 4\pi M_\xi, \tag{5}$$

$$g_0 = \frac{2}{R_\xi^2}\int_0^{R_\xi} \rho d\rho \left[\psi^4 - 2\psi^2 + \left(\frac{d\psi}{d\rho}\right)^2\right].$$

In the case $\psi \ll 1$ and $B = H$ the equations (1) and (2) reduce [13, 14] to a single linear equation

$$\frac{d^2\psi}{d\rho^2} + \frac{1}{\rho}\frac{d\psi}{d\rho} + \left(1 - h_\xi^2\frac{\rho^2}{4}\right)\psi = 0, \tag{6}$$

solutions of which does not depend on $\varkappa$ and can be expressed in terms of the hypergeometric functions (the Kummer functions).

Notice, that in (1)–(5) ξ is chosen as the unity of length, however, one can use $\lambda = \varkappa\xi$ instead, and the field $H_\lambda = \phi_0/(2\pi\lambda^2) = H_\xi/\varkappa^2$ as the unity (or, for instance, $H_\varkappa = \phi_0/(2\pi\lambda\xi) = H_\xi/\varkappa$, or thermodinamic field $H_{cb} = H_\xi/\sqrt{2}\varkappa$). In presenting the results of the calculations (in Sections 3 and 4) we shall use mixed normalization, chosing λ as the unit of length and H_ξ as the unit of field. The results of calculations do not depend on the choice of the concrete numerical algorithm.

3 The state diagram

The solutions $a(\rho)$ and $\psi(\rho)$ of Eqs. (1)–(4) depend on the three parameters: $\varkappa$, R_ξ and h_ξ. The main results of calculations are presented in Fig. 1, where the state diagram of the cylinder is depicted on the plane of the variables $(R_\lambda, \varkappa)$. To every point of this plane

corresponds some solution (or the state) of the system (1)–(4), $\psi(\rho; h_\xi)$ and $a(\rho; h_\xi)$, which shows how the cylinder state at this point changes with the field H. By studying these dependencies one can find five characterictic regions (denoted in Fig. 1 as I_a, I_b, II_a, II_b and II_c) and four critical lines (denoted as π, $S_{\mathrm{I-II}}$, ζ and ζ_i), which merge at the point G into a single curve. This picture is analogous to the state diagram of the plate (see Fig. 1 in Ref. [6]). In the corresponding state diagram of the cylinder (see Fig. 1 in Ref. [8]) the critical lines π and ζ_i are missing, but as a whole this figure is also analogous. To avoid excesive repetitions we refer the reader to Refs. [6, 8] for details. Here we remind only, that every superconducting state can be obtained in two ways: either s-state is reached firstly in the absence of the external field, which then increases (the field increase regime, FI); or the specimen is originally in the n-state (at $T < T_c$) in a strong field, which then diminishes and the specimen passes into the s-state (the field decrease regime, FD). Depending on the chosen regime the different states at the same field H may be realized, i.e. the hysteresis is possible.

[The solutions in FI-regime were found by the iteration method [15], starting with the trial function $\psi(x) = 1.0$; in FD-regime this trial function was chosen as $\psi(x) = 10^{-3}$. Solutions found in this way are stable with relatively small perturbations in their shape. In the hysteresis region there also exists the absolutely unstable branch of solutions (having positive time-increment), which can not be found by our method.]

In FI-regime in regions I_a and I_b in Fig. 1 the Meissner M-state (with $\psi \approx 1$) is completely destroyed by a first order jump to n-state in some field h_1, accompanied by a jump in the cylinder magnetization. In region II_a the M-state is at first partially destroyed (in the field h_1) by a first order jump transformation into a superconducting e-state [9, 10], which finally vanishes by a second order phase transition (in the field h_2). In region II_b the superconductivity is destroyed without jumps by a second order phase transition, however, the magnetization curve, $-4\pi M(H)$, has in this region the inflexion point (the so-called i-states). In region II_c the magnetization vanishes monotonously, having no inflexion points. Thus, the curve $S_{\mathrm{I-II}}$ in Fig. 1 divides the regions of first and second order phase transitions from s- to n-state in FI-regime. (Notice, that in Ref. [8] the asymptote of the curve $S_{\mathrm{I-II}}$ at $R \to \infty$ was found to be $\varkappa_c = 0.92$, instead of $\varkappa_c = 0.94$ for the plate [6]. After recalculating we found these numbers to be $\varkappa_c = 0.93$ in both geometries, as it should be for bulk superconductors).

In the FD-regime in region II_a from the n-state originates firstly the e-state, which transforms then (with the field diminishing) into a metastable (hysteretic) d-state [11], followed by a final jump restorating the M-state. In regions II_b and II_c the hysteresis and the jumps are absent. In region I_b the s-state restores from a supercooled $\overline{n}$-state by a second order phase transition into a hysteretic (metastable) p-state [6] with the following jump into M-state at a field h_r. In region I_a the intermediate p-state does not form and the transition from a supercooled $\overline{n}$-state into M-state happens immediately by a first order jump in a field h_r^*. Thus, the curve π in Fig. 1 marks the boundary where p-states disappear. The curve ζ marks the boundary, above which d-states exist (in region II_a), or $\overline{n}$- and p-states (in region II_b), or only $\overline{n}$-states (in region I_a); above

ζ-line the magnetization jumps exist and hysteresis is possible. Below ζ-line the jumps and hysteresis are impossible, but the inflexion points on the magnetization curves remain (in region II_b). Below ζ_i-line the magnetization vanishes monotonously, having no points of inflexion.

For the readers convenience the characteristic behavior of the magnetization, $-4\pi M(H)$, in different regions of the state diagram is depicted in Fig. 2. One can see here the difference between the states M-, p-, d-, e-. The state p- forms in FD-regime from $\overline{n}$-state (Fig. 2(b)). The state d- forms in FD-regime from e-state (Fig. 2(d)). The marginal μ-state (see Fig. 2(c)) belongs to the critical line $S_{\mathrm{I-II}}$. The difference between p- and d-states vanish on this line, which marks also the points where the supercooled $\overline{n}$-state disappears.

Figs. 3 and 4 illustrate the co-ordinate dependencies $\psi(x)$ and $b(x)$ at different points of the state diagram in different field regimes.

Fig. 3 shows the changes in the space shape of the solutions at the first order jumps in FI-regime. One can see, in particular, that in class-I superconductors (see Figs. 2(a,b) and Figs. 3(a,b) for $\varkappa = 0.8$ and $R_\lambda = 7.5$) the transition from M- to n-state is a first order phase transition (at the field h_1). In class-II superconductors (see Fig. 2(d) and Figs. 3(c,d) for $\varkappa = 1.5$ and $R_\lambda = 4$) the "edge" mechanism of the field penetration into the specimen is realized. Here, out of M-state the e-state forms in a jump [9, 10], having the suppressed values of the order parameter near the cylinder surface, with the external field penetrating into the mesoscopic cylinder through a layer along its boundary. Only later the second order phase transition to the n-state occurs finally (at the field h_2). The dashed line K (with $\psi \ll 1$) matches the linear equation (6) and can be expressed via the Kummer functions.

Fig. 4 illustrates the changes in the space profiles of the solutions $\psi(x)$ and $b(x)$ in FD-regime, when the superconductivity restores from the supercooled $\overline{n}$-state. One can see that in class-I superconductors (see Fig. 2(b) and Figs. 4(a,b) for $\varkappa = 0.8$ and $R_\lambda = 7.5$) the superconductivity nucleates from the $\overline{n}$-state in a second order phase transition (at the field h_p), forming the p-state with $\psi \ll 1$ (the curve K), which developes into the curve p (Fig. 4(a)) and then (at the field h_r) transforms in a jump into the M-state. In class-II superconductors (see Fig. 2(d) and Figs. 4(c,d)), with the field diminishing, the e-state with $\psi \ll 1$ nucleates firstly (the curve K), which then transforms gradually into the d-state (see the curve d in Fig. 4(c)) and passes finally in a jump (at the field h_r) from d- to M-state.

4 The critical fields (the phase diagrams)

When studying the solutions of the GL-equations in different points of the state diagram, one can find, in particular, the critical values of the field at which the transitions between different s- and n-states occur. This is illustrated in Fig. 5.

Fig. 5(a) shows the critical fields, which are found when the representation point $(R_\lambda, \varkappa)$ on the state diagram in Fig. 1 moves along the line $\varkappa = 0.5$. Consider, for

example, the point $R_\lambda = 8$, $\varkappa = 0.5$, which belongs to region I_a in Fig. 1, and look what happens at this point when the field changes (further we denote $h = H/H_\xi$). When the field increases (FI-regime) the superconducting M-state (with $\psi \approx 1$) persists up to point $h_1 = 2.164$ in Fig. 5(a), where the first order jump into n-state ($\psi \equiv 0$) occurs. If the field is now decreased ($h < h_1$, FD-regime), the normal state is conserved and a supercooled (metastable) $\overline{n}$-state exists down to the point h_r^*, where the $\overline{n}$-state becames absolutely unstable and the s-state is restored by a first order jump from $\overline{n}$- into M-state (the field h_r of the jump into M-state is supplied with the index *, if the jump occurs at the point of absolute instability of the $\overline{n}$-state, without forming preliminary the metastable p-state). In the field interval $\Delta_n = h_1 - h_r^*$ the supercooled $\overline{n}$-state coexists simultaneously with the M-state, i.e. the hysteresis is possible. One can see, that with R_λ diminishing the interval Δ_n also diminises and at $R_\lambda = 1.7$ it vanishes completely ($\Delta_n = 0$ at point ζ in Fig. 5(a)). [In Fig. 1 the point ζ corresponds the intersection of the line $\varkappa = 0.5$ in region I_a with the curve ζ, which marks the boundary of the hysteresis states.] The section of the critical curve, which lies below point ζ (in region II_c), corresponds to the hysteresis-less second order phase transitions (here $h_1 = h_r = h_2$, see Fig. 2(f)).

Fig. 5(b) shows the critical fields for the case $\varkappa = 0.8$. Here in FI-regime the M-state loses stability at the field h_1 (at $R_\lambda \gg 1$ the first order phase transition into the n-state occurs). In FD-regime the supercooled $\overline{n}$-state persists down to the field h_p, where the superconducting p-state originates by a second order phase transition; the p-state persists down to the field h_r, where the first order phase transition into the M-state occurs (see Fig. 2(b)). The metastable p-states exist in the field interval $\Delta_p = h_p - h_r$, which vanish at point π in Fig. 5(b) ($R_\lambda = 4.5$). [In Fig. 1 to the point π corresponds the intersection of the line $\varkappa = 0.8$ with the π-boundary of p-states, while to the point ζ ($R_\lambda = 1.9$) corresponds the intersection of the line $\varkappa = 0.8$ with the hysteresis ζ-boundary.] For $\zeta < R_\lambda < \pi$ [in region I_a in Fig. 1] there are no p-states, but in the field interval $\Delta_n = h_1 - h_r^*$ the supercooled $\overline{n}$-state is still possible, which loses stability and transforms into M-state by a first order phase transition, see Fig. 2(a)). For $R_\lambda < \zeta$ (in region II_c) the supercooled $\overline{n}$-state is impossible and the transformation from s- into n-state (and vice-versa) occurs at the critical field $h_1 = h_p = h_r = h_2$ by a second order phase transition (see Fig. 2(f)).

Fig. 5(c) shows the critical fields of the superconductor with $\varkappa = 1$. The line $\varkappa = 1$ in Fig. 1 crosses the the critical curves $S_{\mathrm{I-II}}$, π and ζ in three points: μ_1 ($R_\lambda = 4.4$), π ($R_\lambda = 2.5$) and $\mu_2 = G$ ($R_\lambda = 2.3$). This stipulates the complicated behavior of the critical fields in Fig. 5(c). Indeed, for $R_\lambda > \mu_1$ (in region II_a) the Meissner state in FI-regime loses stability firstly at the field h_1 and passes by a jump into the edge-suppressed e-state, which finally vanishes at the field $h_2 > h_1$ by a second order phase transition into n-state. In FD-regime the e-state reappears at the field h_2, at the field h_1 it transforms smoothly into d-state [11], which exists down to the critical field h_r where the jump into M-state occurs (see Fig. 2(d)). Thus, for $R_\lambda > \mu_1$ the value $\varkappa = 1$ corresponds to the class-II superconductor (using the terminology proposed in Ref. [6]).

In Fig. 5(c) at $\pi < R_\lambda < \mu_1$ (region I_b in Fig. 1) the same value $\varkappa = 1$ corresponds

now to the class-I superconductor. Here the M-state remains stable in FI-regime up to the field h_1, where the first order jump into n-state occurs. In FD-regime a supercooled $\overline{n}$-state appears at first, which persists down to the field $h_p < h_1$, where the p-state originates by a second order phase transition with a subsequent first order jump into M-state at the field h_r (see Fig. 2(b)).

In Fig 5(c) at $G < R_\lambda < \pi$ (region I_a in Fig. 1, where there are no p-states, but $\overline{n}$-state exists) the value $\varkappa = 1$ corresponds again to the class-I superconductor. Here the sequence of the emerging states is shown in Fig. 2(a). [The fields h_1 and h_r^* in Fig. 5(c) differ one from another only slightly and they are indistinguishable in the chosen scale.] For $R_\lambda < G$ the value $\varkappa = 1$ corresponds again to the class-II superconductors (the region II_c); here there is only one critical field h_2, at which M-state passes to n-state (and vice-versa) by a second order phase transition (see Fig. 2(f)). In region II_c there is no hysteresis and no inflexions on the magnetization curves.

Fig. 5(d) shows the critical fields of the superconductor with $\varkappa = 1.2$. For $R_\lambda > \zeta = 2.82$ (region II_a in Fig. 1) the M-state loses stability in FI-regime at the field h_1 and by a jump (j) transforms into e-state, which vanishes finally at the field h_2 (see Fig. 2(d)). In FD-regime (at the field h_2) the e-state reappears again from the n-state, and passes smoothly into the metastable d-state, which ends up at the field h_r by a jump into the M-state (see Fig. 2(d)). The supercooled $\overline{n}$-state in region II_a is impossible. For $\zeta_i < R_\lambda < \zeta$ (region II_b; here $\zeta_i = 1.69$) the magnetization has an inflexion point (i) and two critical fields h_i and h_2 (see Fig. 2(e)). For $R_\lambda < \zeta_i$ (in region II_c) there are no inflexion points and there is only one critical field h_2 (see. Fig. 2(f)).

[Notice, that in the case of a plate [6] (as for a cylinder) below the hysteresis boundary ζ there exist analogous i-states, the boundary ζ_i and the ctritical fields h_i, which are missing in Ref. [6].]

5 Connection with the linearized theory

The critical fields in Fig. 5 were found by a self-consistent solution of the nonlinear GL-equations. However, in case of the second order phase transitions (when $\psi \to 0$) the GL-equations can be linearized [13, 14] and reduced to a single linear equation (6) for ψ, which has the solution expressed (in case of a cylinder) through the hypergeometric Kummer functions. The letter K in Fig. 5 marks the curves of the second order phase transitions, which can be found using the linearized theory. [Notice, that in co-ordinates (R_ξ, h_ξ) the curves K reduce to a single ($\varkappa$-independent) curve, in accordance with Ref. [14]]. One can see, however, that the curve K consists, in fact, of several segments (marked in Fig. 5 by thicker lines), which change with $\varkappa$ and have different meaning in different regions of the state diagram.

Thus, in Fig. 5(a) ($\varkappa = 0.5$) segment h_r^* of the curve K appears in FD-regime and corresponds to the points, where the $\overline{n}$-state ($\psi \equiv 0$) becames absolutely unstable and a first order jump into M-state occurs. Segment h_2 corresponds to the reversible second order phase transitions.

In Fig. 5(b) ($\varkappa = 0.8$) segment h_p of the curve K appears in FD-regime and corresponds to a second order phase transition from $\overline{n}$- into p-state (with $\psi \neq 0$). Segment h_r^* corresponds in FD-regime to the points of absolute instability of $\overline{n}$-states and to a non-reversible first order phase transitions from $\overline{n}$- into M-state. Segment h_2 corresponds to a reversible second order phase transition (s, n).

In Fig. 5(c) ($\varkappa = 1$) the upper segment h_2 of the curve K (which appears in FI-regime) marks the end of e-states and corresponds to a second order phase transition into n-state. Segment h_p appears in FD-regime and corresponds to a second order phase transition from a supercooled $\overline{n}$- into p-state. The lower segment h_2 corresponds to the reversible destruction (or origination) of s-state.

In Fig. 5(d) ($\varkappa = 1.2$) the curve K consists of two segments h_2, with the upper segment marking the boundary of e-states, and the lower – the boundary of existence of the reversible s-states, which have no inflexion points on the magnetization curve.

[The analogous picture of the critical fields exists in the case of a plate [6] (with the hypergeometric Weber functions replacing the Kummer functions). Note also, that in both geometries (for $m = 0$) the superconductivity originates (with $\psi \ll 1$) in the volume, and not only on the specimen surface, see curves K in Figs. 3 and 4.]

The system of nonlinear GL-equations can be reduced to one linear equation also in the case $\varkappa \ll \varkappa_c(R_\lambda)$, $R_\lambda \gg 1$. Indeed, chosing λ as the unit of length and normalizing the potential A by the formula $A(r) = \lambda H_\xi \tilde{a}(x)$, $x = r/\lambda$, one can rewrite Eqs. (1), (2) in the form

$$\frac{d^2\tilde{a}}{dx^2} - \frac{1}{x}\frac{d\tilde{a}}{dx} - \psi^2\tilde{a} = 0, \tag{7}$$

$$\frac{d^2\psi}{dx^2} + \frac{1}{x}\frac{d\psi}{dx} + (\psi - \psi^3) - \varkappa^2\frac{\tilde{a}^2}{x^2}\psi = 0. \tag{8}$$

Neglecting (if $\varkappa \ll 1$) the last term in equation (8) and noticing that $\psi = 1$ in this case is a solution of the problem (for $R \gg 1$), one can rewrite Eq. (7) in the equivalent form

$$\frac{d^2b}{dx^2} + \frac{1}{x}\frac{db}{dx} - b(x) = 0, \quad x = \frac{r}{\lambda}, \tag{9}$$

where $b(x) = x^{-1}d\tilde{a}/dx$ (with $H(r) = r^{-1}dA/dr = H_\xi b(x)$). The solution of equation (9) with the finite value of the field in the origin of co-ordinates is

$$b(x) = b_0 I_0(x), \quad I_0(x) = \sum_{k=0}^{\infty} \frac{1}{k!\Gamma(k+1)}\left(\frac{x}{2}\right)^{2k}, \tag{10}$$

where $I_0(x)$ is the Bessel function of the imaginary argument. The value b_0 can not be found from the linear equation (9), however, the functional dependence of the self-consistent solution for $b(x)$ is described by the formula (10) for all $\varkappa \ll 1$ and $R \gg \lambda$. [In case of a plate with $D \gg \lambda$ the function $I_0(x)$ is replaced by the exponent e^{-x}.]

6 Connection with a thermodinamic field H_{cb}

Among other critical fields in Fig. 5 is also shown a thermodynamic critical field of a bulk superconductor $H_{cb} = \phi_0/(2\pi\sqrt{2}\lambda\xi)$ (in units H_ξ one has $h_{cb} = H_{cb}/H_\xi = (\sqrt{2}\varkappa)^{-1}$). We

stress that this expression for H_{cb} corresponds to a bulk specimen and was found in Refs. [1–5] from thermodynamic considerations, neglecting the role of the boundary effects. The quantity H_{cb} does not enter directly into GL-equations, so the value h_{cb} is a regular point of these equations, bearing no singularity in the behaviour of the solutions.

Recall the meaning of the field H_{cb} [1–5]. According to the energy conservation law, during a first order phase transition from s- into n-state (the Meissner effect) the free energy is absorbed $H_{cb}^2/8\pi$ (for unite volume of infinite superconductor). In the reversed transition from n- into s-state the same energy is discharged. However, as the self-consistent GL-calculations show, in mesoscopic superconductors (plates [6] and cylinders [8, 11]) the energy exchange during (s,n)-transitions is more complicated. Thus, in the case of a cylinder the absorbed (or discharged) energy can be represented as $H_c^2/8\pi$, where the quantity $H_c(R,\varkappa,\nu)$ depends not only on the cyliner radius R and the parameter $\varkappa$, but also on the field regime [$\nu=+1$ in the FI-regime, $\nu=-1$ in FD-regime]. For instance, in a superconducting cylinder with $R_\lambda \gg 1$ and $\varkappa > 0.93$ (region II_a in Fig. 1) the energy in the FI-regime changes in two stages: first, in a field $H_c = H_1$ (i.e. in a field $h_1 = H_1/H_\xi$ in Fig. 5(c) and 5(d)) the energy increases firstly in a jump (at the first order transition from M- to e-state), and then smoothly during the final second order phase transition into n-state at the field $H_2 = H_\xi$ ($h_2 = 1$). In the FD-regime the superconducting energy begins diminishing first smoothly at $h_2 = 1$ and then changes in a jump during the first order transition from d- to M-state at the field h_r.

In a superconducting cylinder with $\varkappa < 0.93$ ($m=0$, $R_\lambda \gg 1$, in regions I_a and I_b in Fig. 1) in FI-regime the specimen absorbs all the energy in a jump (at a field h_1; see Figs. 5(a) and 5(b)). In FD-regime for $0.707 < \varkappa < 0.93$ (in region I_b; see Fig. 5(b)) the energy of a supercooled $\overline{n}$-metal begins diminishing smoothly at a field h_p due to formation of the p-state, then followed by a first order jump at a field h_r at the final restoration of M-state. For $\varkappa < 0.707$ (in region I_a; see Fig. 5(a)) a supercooled metal releases all the energy in a first order jump during the transition from $\overline{n}$- to M-state in the field h_r^*, when the $\overline{n}$-state becomes absolutely unstable.

The above is also illustrated in Fig. 6, where the example of the free energy (Δg) and the magnetic moment ($-4\pi M_\xi$) dependences on the field $h = H/H_\xi$ are given for a cylinder with $R_\lambda = 5$, $\varkappa = 1.5$; the dashed arrows mark the hysteresys loops in FI- and FD-regimes, the dotted arrow corresponds to the point of equilibrium transition between M- and d-states, when their free energies equalize. Evidently, there is no singularity at a thermodynamic field $h_{cb} = 0.47$.

Thus, the value $h_{cb} = (\varkappa\sqrt{2})^{-1}$ is not a critical point for Eqs. (1)–(4). However, there exists an exceptional value $\varkappa = 1/\sqrt{2}$, when the state belongs to the critical line π (at $R_\lambda \gg 1$ in Fig. 1); in this case the solution at $h_{cb} = 1$ posesses special properties (see the next Section).

7 Connection with the Bogomolnyi equations

As is clear from Fig. 1, the region of existence of the metastable p-states is bounded by a π-curve (the states belonging to π-boundary will be named π-states). It is intresting to trace changes in the space profiles of π-states, $\psi(\rho)$ and $b(\rho)$, while moving along π-boundary. This is shown in Fig. 7, where π-solutions are depicted for $R_\lambda = 9,\ 10,\ 12$. One can see, that for $R \gg \lambda$ and $\varkappa \to 1/\sqrt{2}$ the profile of π-states acquires the characteristic shape of the interface between s- and n- half-spaces [1].

Because at $R \to \infty$ the role of the boundary diminishes, the solution $\psi(\rho)$, $b(\rho)$ for a bulk cylinder should go over into the solution $\psi(x)$, $b(x)$ for a bulk plate (at $D \to \infty$). As Bogomolnyi showed [16], for infinite superconductor with $\varkappa = 1/\sqrt{2}$ the GL-equations are degenerate and can be reduced to a system of two nonlinear first order equations, which have an analytic solution. This solution (at $m = 0$ and $H = H_\xi$) is given implicitly by a formula [17]

$$\int_{\psi_i}^{\psi} \frac{dy}{y\sqrt{y^2 - (1 + \ln y^2)}} = x, \quad b_\xi^2(x) = 1 - \psi^2(x), \quad b_\xi(x) = \frac{B(x)}{H_\xi}, \tag{11}$$

where $\psi_i = 0.451$ is the inflexion point [6] of the function $\psi(x)$ ($d^2\psi/dx^2|_{x=0} = 0$, x is a dimensionless Cartesian co-ordinate, $-\infty < x < +\infty$).

The function $\psi(x)$, found according to Eq. (11), is shown in Fig. 7 by a dotted curve. Evidently, the self-consistent solution for ψ at $R_\lambda = 12$ practically coincides with the solution (11) for a bulk plate (the inflexion points i of both solutions are superimposed). The self-consistent solution for a field at $R_\lambda = 12$ is also well described by a formula (11): $b_\xi^2(x) = 1 - \psi^2$. Thus, in case of a bulk cylinder (at $m = 0$, $\varkappa = 1/\sqrt{2}$, $H = H_\xi$, $R_\lambda \to \infty$), as well as for a bulk vortex-free plate [6], the degenerate Bogomolnyi solution corresponds to a metastable π-state (i.e. to the last of p-states, existing in FD-regime in region I_b in Fig. 1).

8 Conclusions

In conclusion, we clarify why there exist two critical parameters, $\varkappa_0 = 0.707$ and $\varkappa_c = 0.93$, which (according the GL-theory) divide bulk superconductors (the plates, or cylinders) into two different groups. As was mentioned already, there are two regimes of the field action on the superconductor: the field increase (FI) and the field decrease (FD) regimes. In FI-regime the value $\varkappa_c = 0.93$ corresponds to the point of absolute instability of a superconducting phase, when the M-state either passes immediately into n-state (class-I superconductors with $\varkappa < \varkappa_c$), or the tail of e-states forms preliminary (class-II superconductors with $\varkappa > \varkappa_c$; see Fig. 2). In FD-regime the value $\varkappa_0 = 0.707$ correspondsto the point of absolute instability of a supercooled normal phase, when the $\overline{n}$-state either passes immediately into the M-state (type-I superconductors with $\varkappa < \varkappa_0$), or the intermediate p-state forms preliminary (type-II superconductors with $\varkappa > \varkappa_0$; see Fig. 2). Thus, two critical parameters ($\varkappa_0$ and $\varkappa_c$) reflect the possibility of the hysteresis

and the existence of different physical processes, which take place in the system. One can also say, that the value $\varkappa_c$ divides bulk superconductors into two classes in FI-regime and corresponds to the maximal field (H_ξ) of the existence of a superconducting M-state. The value $\varkappa_0$ divides bulk superconductors into two types in FD-regime and corresponds to the minimal field (H_ξ) of the existence of a supercooled $\overline{n}$-state. Finally, two critical parameters $\varkappa_0$ and $\varkappa_c$ describe two different regimes of the field action, they both have clear physical significance.

We also clarify the reason, why the maximal critical field for the existence of superconductivity ($H_{max} = H_\xi$) coincides with the minimal critical field for the existence of a supercooled $\overline{n}$-state ($H_{min} = H_\xi$). The point is that both of these fields correspond to the s-states (e- or p-) with $\psi \ll 1$, and both are described by the same $\varkappa$-independent linear equation (6) [13, 14]. However, these two formulas correspond to different $\varkappa$ ($H_{max} = H_\xi$ for $\varkappa > \varkappa_c$ in FI-regime, and $H_{min} = H_\xi$ for $\varkappa < \varkappa_c$ in FD-regime), i.e. they describe different superconductors with different values of $\lambda = \varkappa\xi$. Since neither the amplitude nor the transition point can be found from the linear equation as functions of $\varkappa$, it is clear, that the critical value $\varkappa_c$ (as well as $\varkappa_0$) should be found from a set of general nonlinear equations.

That the value $\varkappa_0 = 1/\sqrt{2}$ corresponds to the boundary of the metastable p-states in FD-regime, was not mentiond by Ginzburg and Landau [1] because they considered the infinite system, where the superconductor's boundaries are beyond the field of vision. Subsequently the question about the external field and how it changes can not be formulated. It turns out, that in a finite dimension system [6] the model superconducting state, which has the form of the (s, n)-interface [1], cannot be realized simply by increasing the external field. It would be necessary to use FD-regime and pass through the sequence of a supercooled metastable $\overline{n}$- and p-states, the last of which (at $\varkappa = \varkappa_0$ and $H = H_\xi$) would correspond to the (s, n)-interface [6]. [Actually, in Ref. [1] the intermediate state of a bulk type-I superconductor was considered, with the field directed perpendicular the surface of the plate, while in Ref. [6] the field is directed parallel to the surface of the plate.]

Note also, that during first order jumps (which occur at the instability points h_1 and h_r) the superconducting states change in time. Such nonstationary processes must be accompanied by splashes of electromagnetic and phonon radiation [18], which (in principle) can be detected experimentally. Besides, it is possible (in principle) to observe the magnetization jumps in transitions between different vortex-free states of mesoscopic superconductor, and also the heat capacity jumps and various hysteresis phenomena. However, the detailed discussion of the experiments is beyond the scope of the present investigation. We intended only to expose the GL-theory predictions, using the one-dimensional solutions of GL-equations (in case $m = 0$). Such one-dimensional approach was used in a number of publications [19–21] to describe also the vortex states with $m \neq 0$. However, some of the questions raised in these papers require further attention and we intend to discuss the case $m \neq 0$ in more detail in future.

Evidently, the described above e-layer with a suppressed value of the order parameter

(which forms in superconductors with $\varkappa > \varkappa_c$) would become unstable (if the cylinder radius R is large) and break into separate vortices (having $\psi = 0$ at each of the vortex axises), so in the increasing field H the regular vortex lattice would form [2]. Thus, the one-dimensional centrally disposed vortex states can be realized, probably, only in sufficiently small size superconductors. However, for a detailed description of a more complicated two-dimensional states (with $m > 0$) it would be necessary to solve partial differential equations. This would require a specific methods of investigation and large computers. [See for instance papers [22, 23], where the two-dimensional solutions were found numerically to describe the experiments [24–28] with a thin superconducting disks in a perpedicular magnetic field.] Further study of the topics touched above is needed both theoretically and experimentally.

Acknowledgements

I am grateful to V.L. Ginzburg for his interest in this work and valuable comments, and also to V.G. Zharkov, A.Yu. Tsvetkov, N.B. Konukhova and A.L. Dyshko for useful discussions. This work was supported through the grant RFFI 02-02-16285.

References

[1] V.L. Ginzburg and L.D. Landau: "To the theory of superconductivity", *Zh.Exp.Teor.Fyz.*, Vol. 20, (1950), pp. 1064–1082.

[2] A.A. Abrikosov: *Fundamentals of the Theory of Metals*, North-Holland, Amsterdam, 1988.

[3] M. Tinkham: *Introduction to Superconductivity*, McGraw Hill, New York, 1975.

[4] P.G. deGennes, *Superconductivity of Metals and Alloys*, Addison-Wesley, New York, 1989.

[5] D. Saint-James, G. Sarma, E.J. Thomas, *Type II superconductivity*, Pergamon, Oxford, 1969.

[6] G.F. Zharkov: "First and second order phase transitions and magnetic hysteresis in a superconducting plate", *J.Low Temp.Phys.*, Vol. 130, (2003), pp. 45–67.

[7] A.Yu.Tsvetkov, G.F. Zharkov, V.G. Zharkov: "Superconducting plate in a magnetic field", *Krat. Soob. Fyz. FIAN*, Vol. 2, (2003), pp. 42–50.

[8] G.F. Zharkov, V.G. Zharkov, A.Yu. Tsvetkov: "GL-calculations for superconducting cylinder in a magnetic field", *Phys.Rev.B*, Vol. 61, (2000), pp. 12293–12312.

[9] G.F. Zharkov: "The emergence of superconductivity and hysteresis in a type-I superconducting cylinder", *Zh.Exp.Teor.Fyz.*, Vol. 122, (2002), pp. 600–609.

[10] G.F. Zharkov, V.G. Zharkov, A.Yu. Tsvetkov: "Self-consistent solutions of GL-equations and superconducting edge-states in a magnetic field", *Krat. Soob. Fyz. FIAN*, (2001), pp. 35–48; "One-dimensional solutions of GL-equations for superconducting cylinder in magnetic field", ibid, N 12, pp. 31–38 (2001).

[11] G.F. Zharkov: "Transitions of I- and II-order in magnetic field for superconducting cylinder obtained from self-consistent solution of GL-equations", *Phys.Rev.B*, Vol. 63, (2001), pp. 224513–224519.

[12] V.L. Ginzburg: "The destruction and onset of superconductivity in magnetic field", *Zh.Exp.Teor.Fyz.*, Vol 34, pp. 113–125.

[13] D. Saint-James, P. deGennes: "Onset of superconductivity in decreasing field", *Phys.Lett.*, Vol. 7, (1963), pp. 306–308.

[14] D. Saint-James: "Etude du champ critique H_{c3} dans une geometrie cylindrique", *Phys.Lett.*, Vol. 15, (1965), pp. 13–15.

[15] G.F. Zharkov and V.G. Zharkov: "Magnetic vortex in superconducting wire", *Physica Scripta*, Vol. 57, (1998), pp. 664–667.

[16] E.B. Bogomolnyi: "Stability of classical solutions", *Yad.Phys.*, Vol. 24, (1976), pp. 861–870.

[17] A.T. Dorsey: I. Luk'yanchuk, "Theory of superconductors with $\varkappa$ close to $1 sqrt 1/2$", Phys.Rev.B, Vol. 63, (2001), pp. 174504–174517; *Ann.Phys.(N.Y.)*, Vol. 233, (1993), pp. 243.

[18] A.M. Gulian and G.F. Zharkov: *Nonequilibrium Electrons and Phonons in Superconductors*, Kluwer/Plenum, New York, 1999.

[19] H.J. Fink and A.G. Presson: "Superheating of the Meissner state and the giant vortex state of a cylinder of finite extent", *Phys.Rev.*, Vol. 168, (1968), pp. 399–402.

[20] H.J. Fink, D.S. McLachlan and B. Rothberg-Bibby: "First and second order phase transitions in moderately small superconductors in a magnetic field", In: Prog. in Low Temp. Phys.", (Ed.): Vol. VIIb, D.F. Brewer North Holland, Amsterdam, 1978, pp. 435–516.

[21] G.F. Zharkov: "Paramagnetic Meissner effect in superconductors from self-consistent solution of GL-equations", *Phys.Rev.B*, Vol. 63, (2001), pp. 214502–214509.

[22] F.M. Peeters et. al: *Superlatt. and Microstruct.*, Vol. 25, (1999), pp. 1195; "Hysteresis in mesoscopic superconducting disks", *Phys.Rev.B*, Vol. 59, (1999), pp. 6039–6042; "Vortex structure of thin mesoscopic disks with enhanced surface superconductivity", *ibid*, Vol. 62, (2000), pp. 9663–9687; "Superconducting properties of mesoscopic cylinders with enhanced surface superconductivity", *ibid*, Vol. 65, (2002), pp. 024510(10).

[23] J.J. Palacios: "Vortex matter in superconducting mesoscopic disks", *Phys.Rev.B*, Vol. 58, (1998), pp. R5948–R5951; "Flux penetration and expulsion in thin superconducting disks", *Phys.Rev.Lett.*, Vol. 83, (1999), pp. 2409–2412; "Stability and paramagnetism in superconducting mesoscopic disks", *Phys.Rev.Lett.*, Vol. 84, (2000), pp. 1796–1880.

[24] V.V. Moshchalkov et al.: "Effect of sample topology on the critical fields of mesoscopic superconductors", *Nature*, Vol. 373, (1995), pp. 319–322; "Symmetry-induced formation of antivortices in mesoscopic superconductors", *Nature*, Vol. 408, (2000), pp. 833–835.

[25] A.K. Geim et. al.: "Phase transitions in individual sub-micrometer superconductors", *Nature*, Vol.390, (1997), pp. 259–262; "Paramagnetic Meissner effect in small superconductors", *Nature*, Vol. 396, (1998), pp. 144–146; "Non-quantized penetration of magnetic field in the vortex state of superconductors", *Nature*, Vol. 407,

(2000), pp. 55–57; "Fine structure in magnetization of individual fluxoid states", *Phys.Rev.Lett.*, Vol. 85, (2000), pp. 1528–1532.

[26] D.S. McLachlan: "Quantum oscillations and the order of the phase charge in a low $\varkappa$ type-II superconducting microcylinder", *Solid State Commun.*, Vol. 8, (1970), pp. 1589–1593; "(II) Quantum oscillations, pinning and the superheating and other critical fields in a low $\varkappa$ type-II superconducting microcylinder", *ibid*, pp.1595–1599.

[27] O. Buisson et al.: "Magnetization oscillations of a superconducting disk", *Phys.Lett.A*, Vol. 150, (1990), pp. 36–42.

[28] F.B. Műller-Allinger, A.C. Motta: "Paramagnetic reentrant effect in high puruty mesoscopic AgNb proximity structure", *Phys.Rev.Lett.*, Vol. 84, (2000), pp. 3161–3164.

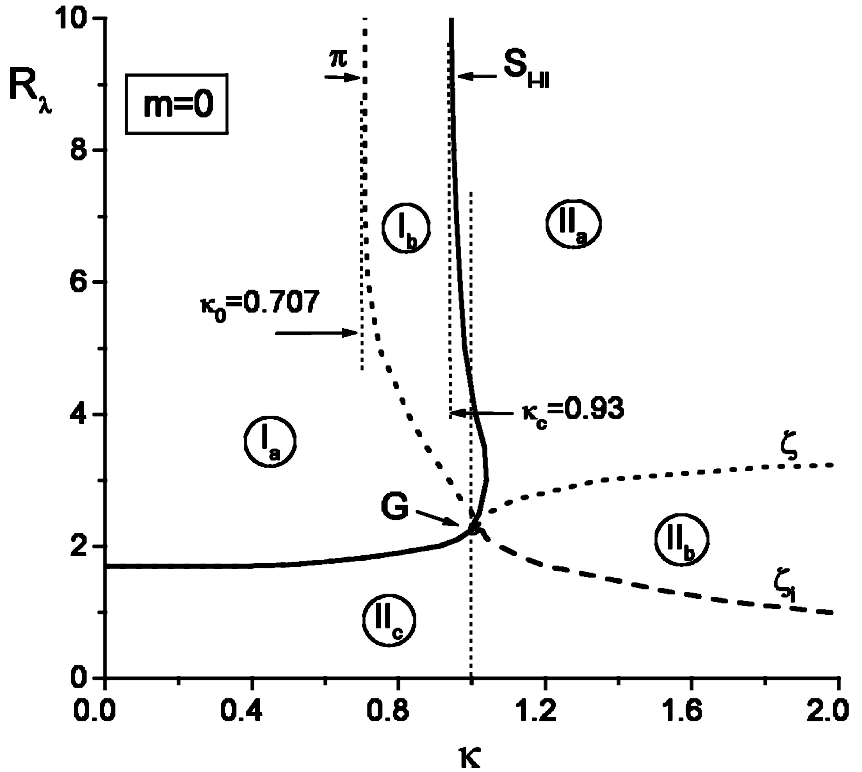

Fig. 1 The state diagram on the plane $(R_\lambda, \varkappa)$. Curve $S_{\mathrm{I-II}}$ marks the boundary between the first and second order phase transitions in FI-regime; curve π marks the boundary of p-states in FD-regime. Above curve ζ (in region II_a) the jumps of magnetization exist at transitions between M-, e- and d-states and the hysteresis is possible; below curve ζ no hysteresis or jumps are possible. In region II_b the magnetization curves $M(H)$ have the inflexion points; in region II_c there are no inflexion points.

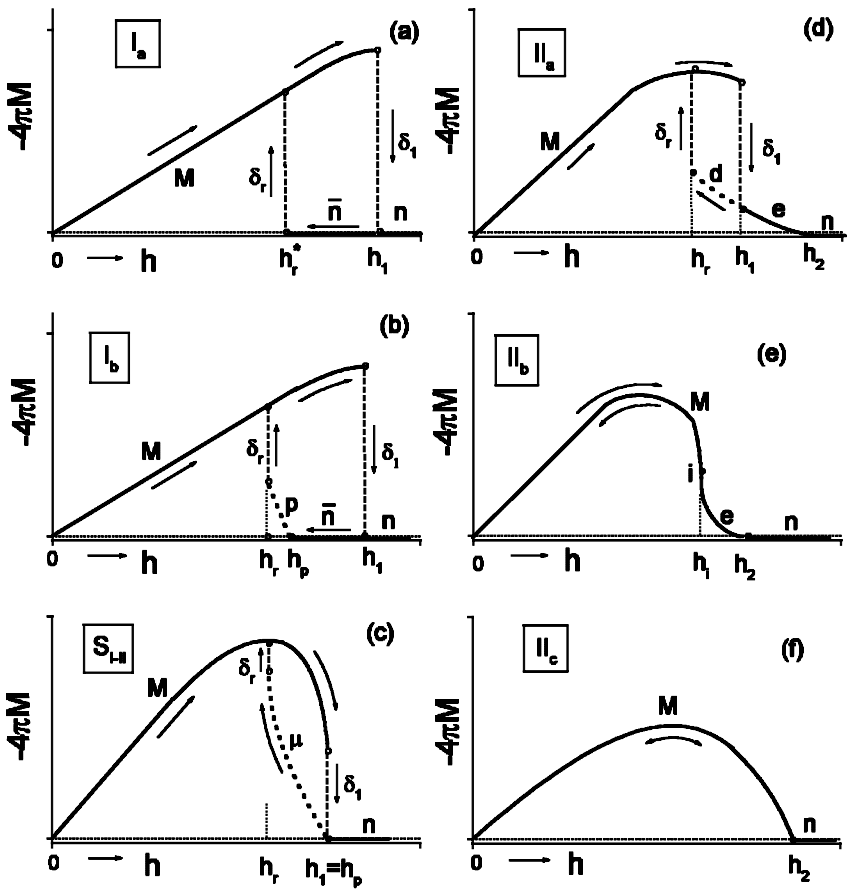

Fig. 2 The magnetization $(-4\pi M)$ as a function of the field h (schematically) in different regions of the state diagram: (a) – I_a; (b) – I_b; (c) – $S_{\mathrm{I}-\mathrm{II}}$-boundary; (d) – II_a; (e) – II_b; (f) – II_c. Shown are the states (M, n, $\overline{n}$, p, e, d), the critical fields (h_1, h_2, h_p, h_r) and jumps (δ_1, δ_r) at the points of transition between the states. The arrows mark the hysteresis loops in FI- and FD-regimes. The letter i in Fig. 2(e) marks the inflexion point of the hysteresis-less curve. In region II_c (Fig. 2(f)) the inflexion points are absent. (The field normalization is arbitrary.)

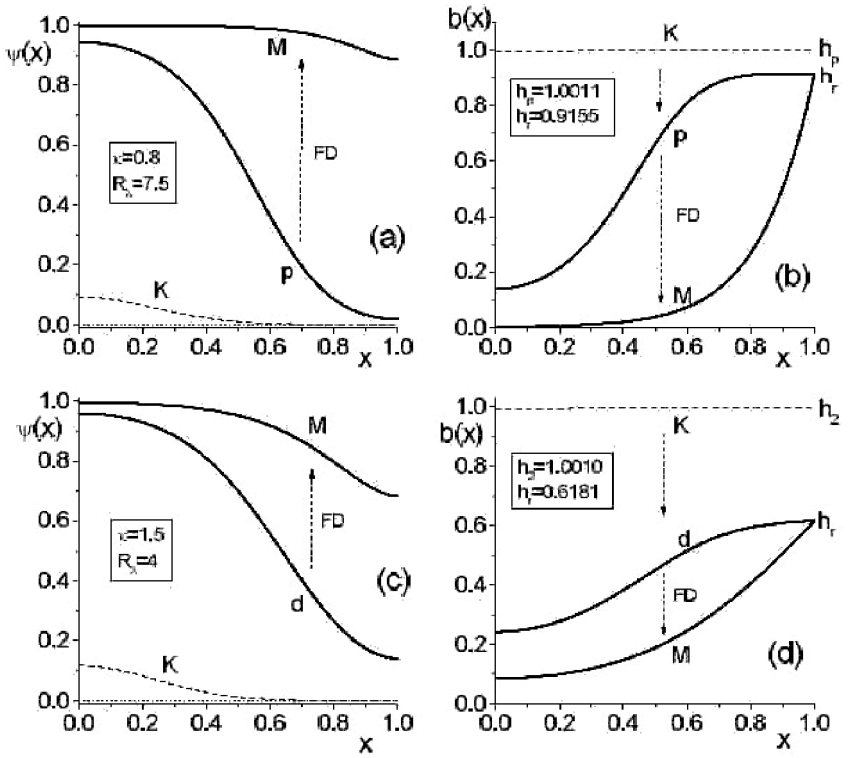

Fig. 3 The changes of the solutions $\psi(x)$ and $b(x)$ ($x = r/R$) in the field increase regime (FI). (a) and (b) – for $\varkappa = 0.8$, $R_\lambda = 7.5$ (region I_b in Fig. 1); at $h_\xi = 1.2316$ the jump occurs from M- to n-state. (c) and (d) – for $\varkappa = 1.5$, $R_\lambda = 4.0$ (region II_b in Fig. 1); at $h_\xi = 0.6488$ the jump occurs from M- to e-state, which vanish finally in a field $h_\xi = 1.0098$ by a second order phase transition. The dashed curve K corresponds to e-state with $\psi \ll 1$ ($h_\xi = 0.9956$) and it can be described by the Kummer function.

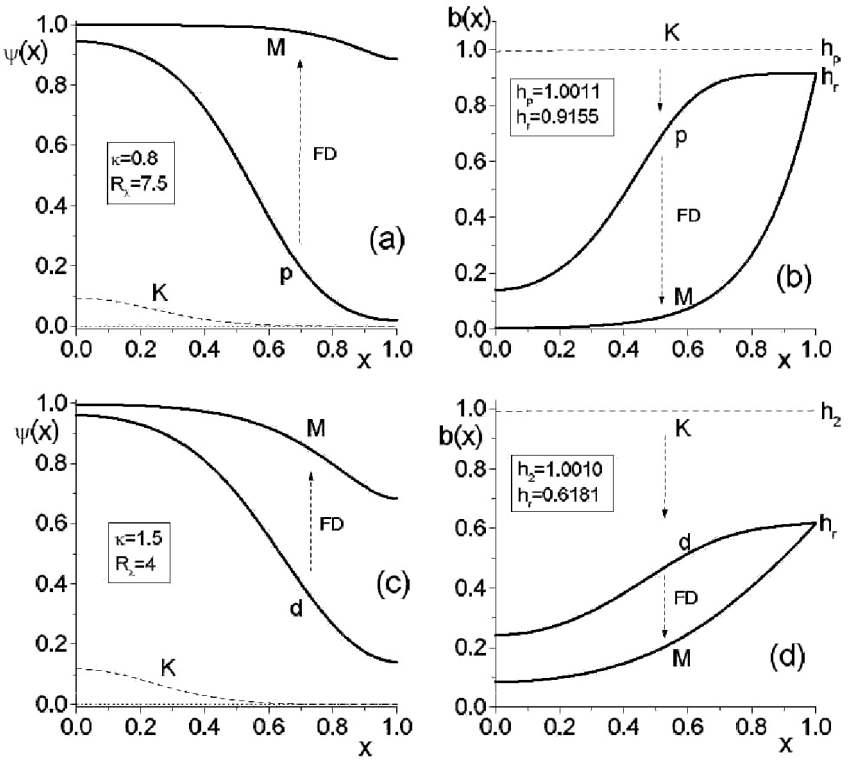

Fig. 4 The changes of the solutions $\psi(x)$ and $b(x)$ ($x = r/R$) in the field decrease regime (FD). (a) and (b) – for $\varkappa = 0.8$, $R_\lambda = 7.5$ (region I_b in Fig. 1); at $h_\xi = 0.9155$ the jump occurs from p- to M-state. The dashed curves K correspond here to p-state with $\psi \ll 1$ ($h_\xi = 1.0$), which begins nucleating at $h_p = 1.0011$. (c) and (d) – for $\varkappa = 1.5$, $R_\lambda = 4.0$ (region II_b in Fig. 1); at $h_\xi = 0.6181$ the jump from d- to M-state occurs. The dashed curves K correspond here to e-state with $\psi \ll 1$ ($h_\xi = 0.9956$), which begins nucleating at $h_2 = 1.0098$.

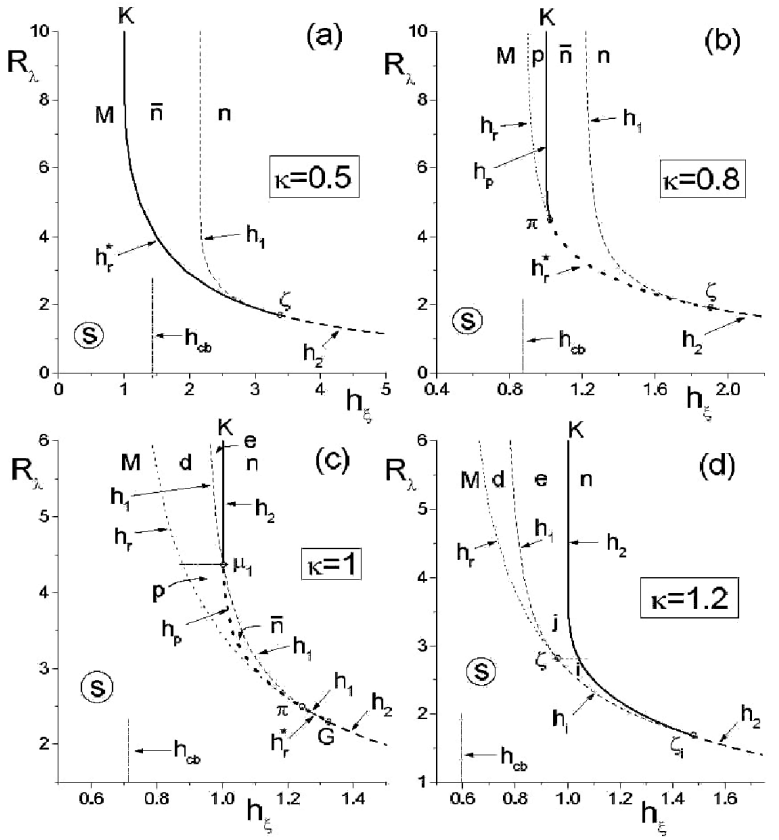

Fig. 5 The critical fields versus cylinder radius R_λ ($m = 0$) in cases: (a) $\varkappa = 0.5$; (b) $\varkappa = 0.8$; (c) $\varkappa = 1$; (d) $\varkappa = 1.2$; $h = H/H_\xi$. The critical fields (h_1, h_2, h_p, h_i, h_r, h_r^*) mark points of transition between different states (M, e, d, i, n, $\overline{n}$) in FI- and FD-regimes (see the text). The letter K marks the curve of a second order phase tansitions, which can be found from a linearized theory.

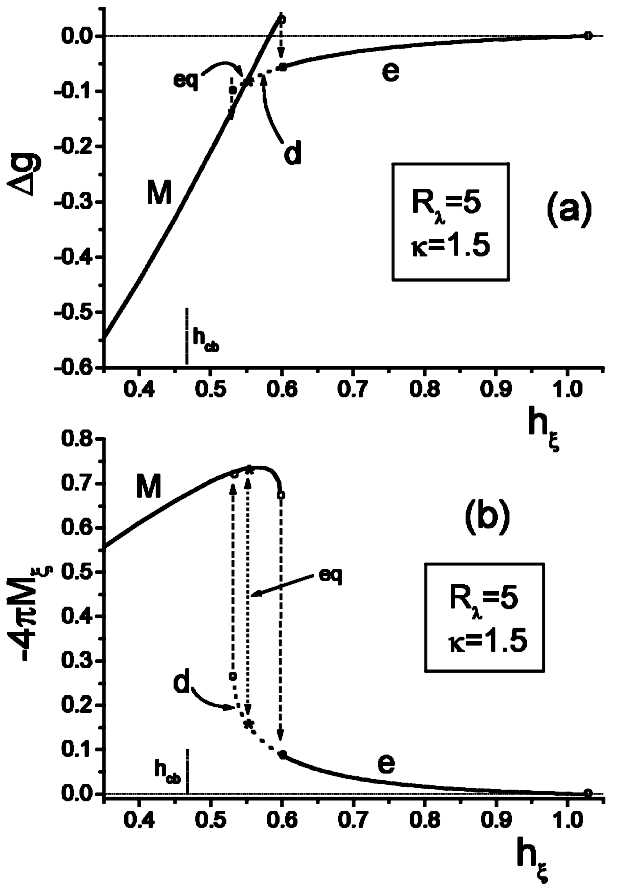

Fig. 6 The Gibbs free energy (a) and magnetization (b) of the cylinder with $R_\lambda = 5$, $\varkappa = 1.5$ as function of $h = H/H_\xi$. The arrows mark the transitions from M- to e-state ($h_1 = 0.60$, FI-regime) and from d- to M-state ($h_r = 0.53$, FD-regime). The sign * marks the crossing point of the free energy curves (the equilibrium points, eq, $h_{eq} = 0.55$), where, according to the thermodynamics, the magnetization jump in FD-regime should occur. Thermodynamic field $h_{cb} = (\varkappa\sqrt{2})^{-1} = 0.47$ is also marked.

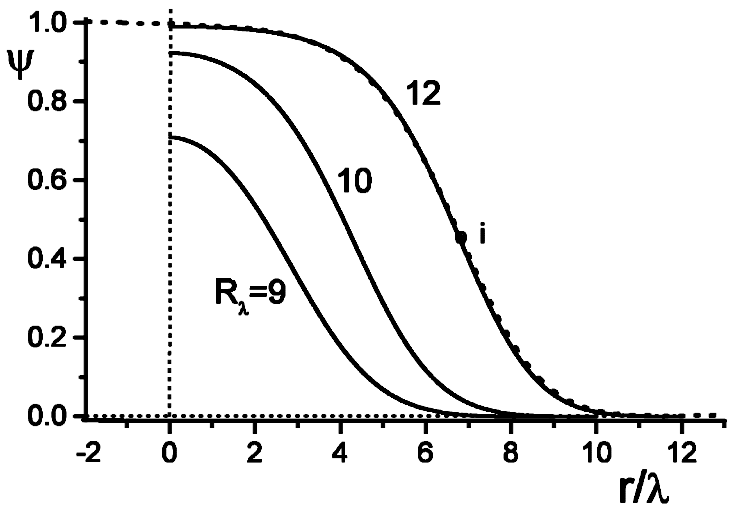

Fig. 7 The self-consistent π-solutions $\psi(x)$ for $R_\lambda = 9$ ($\varkappa = 0.7077$, $h = H/H_\xi = 0.999$), $R_\lambda = 10$ ($\varkappa = 0.7075$, $h = 0.999$) and $R_\lambda = 12$ ($\varkappa = 0.7075$, $h = 0.999$). The dotted line is the degenerate Bogomolnyi solution (the inflexion points i of the degenerate solution (11) and of the self-consistent solution with $R_\lambda = 12$ are superimposed).